

Movie S1. Image sequence showing output of the ‘attached’ Cytosim simulation of melanosome transport in melanocytes see main text and Figure 9 for details. Companion to Figure S11A. Acquisition frame rate 0.5 sec⁻¹. Playback frame rate 5 sec⁻¹.

Movie S2. High magnification detail from movie 1 showing the melanosome and actin filament movements in a small area of a model cell (melanosomes are shown individually coloured in order to aid tracking of individuals over time). This region corresponds to the red boxed region shown in the overview images in Figure S11B. Companion to Figure S11B. Acquisition frame rate 0.5 sec⁻¹. Playback frame rate 5 sec⁻¹.

Movie S3. Image sequence showing output of the ‘unattached’ Cytosim simulation of melanosome transport in melanocytes see main text and Figure 9 for details. Companion to Figure S11A. Acquisition frame rate 0.5 sec⁻¹. Playback frame rate 5 sec⁻¹.

Tables

Table S1. The complete list of genes targeted by siRNA knockdown in melanocytes in this study.

Gene Symbol	Accession # (NM_)	Gene Symbol	Accession # (NM_)	Gene Symbol	Accession # (NM_)
Actg1	NM_009609.2	Rac1	NM_009007.2	inf2	NM_198411
Iqgap1	NM_027711.1	Rac2	NM_009008.3	arpc1a	NM_019767
Pfn1	NM_011072.4	Rac3	NM_133223.4	WASp	NM_009515
Msn	NM_010833.2	RhoBTB1	NM_001252638.1	N-WASp	NM_028459
Myh9	NM_022410.2	RhoBTB2	NM_153514.5	wave1	NM_031877
Rhoc	NM_007484.2	RhoBTB3	NM_028493.2	wave-2	NM_153423
Sep-02	NM_001159719.1	RhoH	NM_001081105.1	wave-3	NM_145155
Mtpn	NM_008098.4	Rnd1	NM_172612.3	wash	NM_001037
Tln1	NM_011602.5	Rnd2	NM_009708.1	whamm	NM_00100418
Capzb	NM_001037761.2	RhoD	NM_007485.4	jmy	NM_021310
Cotl1	NM_028071.3	IQgap2	NM_027711.1	cortactin	NM_007803
Coro1c	NM_011779.3	Actr2	NM_146243.2	HCLS1	NM_008225
Myl6b	NM_172259.1	Arp3	NM_023735.2	COBL	NM_172496
Tmod3	NM_016963.2	Arpc5	NM_026369.2	lmod1	NM_053106
Actr3	NM_023735.2	Arpc4	NM_026552.3	lmod2	NM_053098
Zyx	NM_011777.2	Arpc2	NM_029711.1	lmod3	NM_001081157
Dstn	NM_019771.2	Arpc3	NM_019824.3	ctnna2	NM_145732
Epb4.1l3	NM_013813.1	Tagln2	NM_178598.2	ctnna1	NM_009818
Epb4.1l2	NM_001199265.1	Flna	NM_010227.2	ctnna3	NM_001164376

Ppp1cc	NM_013636.3	Dsp	NM_023842.2	ctnnb1	NM_007614
Rap2b	NM_029519.3	Ptma	NM_008972.2	cdh1	NM_009864
Cdc42	NM_001243769.1	Tpm1	NM_001164256.1	cdh2	NM_007664.4
MYOVA	NM_010864.2	Cfl1	NM_007687.5	cdh3	NM_001037809
Vasp	NM_009499.2	Actb	NM_007393.3	Lrrc58	NM_177093
Enah	NM_010135.2	Diap1	NM_007858.2	acta1	NM_009606
Diap2	NM_172493.2	Diap3	NM_019670.1	actg2	NM_009610
FMNL3	NM_011711.1	FMNL1	NM_019679.2	actc1	NM_009608
DAAM1	NM_026102.2	FMNL2	NM_172409.2	acta2	NM_007392
DAAM2	NM_001008231.2	FHOD1	NM_177699.4	actbl2	NM_175497
FMN1	NM_010230.2	FHOD3	NM_175276.3	rab27a	NM_023635
FMN2	NM_019445.2	RhoB	NM_007483.2	jup	NM_010593
RhoA	NM_016802.4	ROCK2	NM_009072.2	ctnnd	NM_001085448
Rif	NM_175092.3	RhoJ	NM_023275.2	vcl	NM_009502
ROCK1	NM_009071.2	RhoG	NM_019566.3	vim	NM_011701
Spire1	NM_194355.2	Rnd3	NM_028810.2	Nckipsd	NM_030729
Spire2	NM_172287.2	Arcp1b	NM_023142.2	gsl	NM_146120
RhoQ	NM_145491.2	Lmo2	NM_001142336.1	coro6	NM_139128
RhoU	NM_133955.4	grid2ip	NM_133355	coro1a	NM_009898
RhoV	NM_145530.2	fhd1	NM_001033301	coro1b	NM_011778

Gene Symbol	Accession # (NM_)
coro2a	NM_178893
wipf1	NM_153138
nckbeta	NM_010879
pak1	NM_011035
Tmod1	NM_021883
tmod2	NM_001038710
tmod4	NM_016712
tpm2	NM_009416
tpm3	NM_022314
tpm4	NM_001001491

Table S2: Rab27a unique peptides identified using mass spectrometry at $\geq 95\%$ confidence level in anti-Rab27 immunoprecipitates.

Confidence %	Sequence	Modifications	Protein Modifications	Cleavages	Obs MW	z
99	DAMGFLLLFDLT NEQSFLNVR	Carbamido methyl @N-term			2499.2451	3
99	FITTVGIDFR				1167.6279	2

99	FLALGDSGVGK	Carbamido methyl @N-term			1119.5885	2
99	FLALGDSGVGK				1062.5676	2
99	IHLQLWDTAGQER				1565.7892	3
99	LQLWDTAGQER	Carbamido methyl @N-term		cleaved H-L@N-term	1372.6766	2
99	LQLWDTAGQER			cleaved H-L@N-term	1315.6528	2
99	SDGDYDYLIK	Acetyl@N-term	Acetyl@2	cleaved M-S@N-term	1229.5472	2
99	SLTTAFFR				941.4979	2
99	SNGHTSADQLSEEK	Ammonia-loss(N)@2			1484.6572	2
99	TSVLYQYTDGK				1273.6177	2
99	SWIPEGVVR				1041.5584	2
99	ANGPDGAVGR				912.4656	2

Table S3: SPIRE1 unique peptides (human) identified using mass spectrometry at ≥95% confidence level in anti-Rab27 immunoprecipitates.

Confidence (%)	Sequence	Modifications	Cleavages	Obs MW (Da)	z
99	ALFAETMELHTFLTK			1750.889	3
99	APTLAELDSSESEETLHK			2084.971	3
99	DALSLEEILR			1157.628	2
99	DGAVTLAPAADDAGEPPPVAGK			2018.018	2
99	ENGLSTSQQVPAQR			1513.742	2
99	ENGLSTSQQVPAQR	Deamidated(N)@2		1514.732	2
99	EPGAAGGAAGGSR			1056.495	2
99	FLPISSTPQPER			1370.713	2
99	FWVQVMR			964.5029	2
99	LCAAHLPTESDAPNH YQAVCR	Carbamido methyl(C)@2 Carbamido methyl(C)@20		2409.098	4
99	LPSKPYSTLPIFSLGPS ALQR			2271.262	3
99	NLVESSMVNGGLTSQTK	Deamidated(N)@9		1764.897	2
99	SAHEIILDFIR			1312.713	2
99	SDESSTDLEELK			1351.599	2

99	SMDKSDEELQFPK		missed K-S@4	1552.695	3
99	STLPIFSLGPSALQR		cleaved Y-S@N-term	1585.882	2
99	STSSSSVSPSFPEEPVL EAVSTR			2379.126	3
99	TEAVGGEGPR			971.4687	2

Table S4. The sequences of siRNA oligonucleotides used in this study.

siRNA name	Sense oligonucleotide sequence 5'-3'
SPIRE1#1	GGAAACACCUACGAACGUG
SPIRE1#2	GAAAUUAGACGGAGCAGAC
SPIRE1#3	GGACGACAUUCGUGCAAA
SPIRE1#4	GCAUACAUUUCUGACCAAA
SPIRE2#1	GGACGCACAUGAACUUAUC
SPIRE2#2	GAGCGUGGAUGUCCUCAAU
SPIRE2#3	CAAGAAGUAUGGACACAUC
SPIRE2#4	CAAAGAACACUGCACGAGA
Formin-1#1	GGACAAACCUGAACAAUUU
Formin-1#2	GAACGUGCCCAGUGCAUAA
Formin-1#3	GCAGACGGAUUAUAGUUUAG
Formin-1#4	GGUGAGCACGCAUUAGUAA
Rab27a	UUGAGAAUCCAGAUUUCAA
NT	UAAGGCUAUGAAGAGAUAC

Table S5. The sequences of taqman primers and probes used in this study.

Target	Sense strand primer 5'-3'	Reverse strand primer 5'-3'	Probe 5'-3'

GAPDH	GTGTCCGTCGTGGATCTGA	CCTGCTTCACCACCTTCTTGA	CCGCCTGGAGAAACCTGCC AAGTATG
SPIRE1	GGCTATGTATTATCTGTTTG AGAGAGCTT	CCAGGACCTGACGGATGTG	AACCCTCAAAGGAGGAATT CTGCTACCCA
SPIRE2	TCCGTGCCAGGAACTATAA GCT	GATAAGTTCATGTGCGTCCTT CTTC	CAAGGTCATGGTCGATG

Table S6. Primers and control templates used in qRT-PCR experiments.

Target	Sense strand primer 5'-3'	Reverse strand primer 5'-3'	Template
SPIRE1	AGGATGAAGGGTACGAGGCT	CTGATAATGATTGGGTGCCTCC	pAcGFP-C1-mm-SPIRE1 (Full-length murine SPIRE1 (XM_006526207.3), as a C-terminus fusion to GFP)
SPIRE2	ACACTGCACGAGAAGATCCT	ACTTGATGTCCCCAGAGCAG	pAcGFP-C1-mm-SPIRE2 (Full-length murine SPIRE2 (AJ459115), as a C-terminus fusion to GFP)
FMN1	AGCTGGTGTGCAAGGAGTCC	GCTGGGGGTGACCTCCTTCT	pcDNA3-mm-FMN1-FH2 (FH2 domain of murine FMN1 XM_011239295.2)
FMN2	TTCACAGGGGAGAACACTGCT	ACTGCCCTTCGCTGTAATCC	pEGFP-C1-mm-FMN2 Full-length murine FMN2 (NM_019445.2), as a C-terminus fusion to EGFP)
Mlph	TTGAACAAGCGAATGTCAGCTG TGG	GAGTGTCTCCTCCTCTGTGTCAGC A	pAcGFP1-C1-mm-Mlph (aa 2 - 466 of murine Mlph (NM_053015.3),

			as a C-terminus fusion to GFP)
--	--	--	--------------------------------

Table S7. Primary antibodies used in this study.

Antibody	Supplier	Catalogue code	Dilution/ Concentration (application)	Figure
Rabbit anti-FMN1	Markus Dettenhofer (CEITEC - Central European Institute of Technology, Brno, Czech Republic.)	¹	1:1000 (immunoblot)	1d
Goat anti-GAPDH	Sicgen	Ab0049-200	1:5000 (immunoblot)	1d, S4c
Goat anti-GFP	Sicgen	AB0020-200	1:1000 (immunoblot)	S4
Rabbit anti-GFP	TakaraBio/Clontech	632376	1µg/ml (immunoblot)	6e S5c S6
Mouse monoclonal anti-c-Myc (9E10)	Santa Cruz Biotechnology	sc40	0.4µg/ml (immunoblot)	6b, 6c
Mouse monoclonal anti-TRP1 (Ta99)	Santa Cruz Biotechnology	sc-58438	1:1000 (immunofluorescence)	S8b
Mouse monoclonal anti-GFP IgG1κ (clones 7.1 and 13.1)	Sigma-Aldrich	11814460001	1:300 (immunofluorescence), 1:1000 (immunoblot)	1f, 1g, 4b, 5b, 7, 8b, S1g, S3b, S5e, S9a, S10b, S10d
Mouse-anti-human HSP90	Santa Cruz, Biotechnology.	sc-69703	1:1,000 (immunoblot)	S10d
Rabbit-anti-human ARL1	Proteintech.	16012-1-AP	1:2,000 (immunoblot)	S10d

Table S8. Secondary antibodies used in this study.

Antibody	Conjugate	Supplier	Catalogue code	Dilution/ Concentration (application)	Figure
Donkey anti-Rabbit IgG	IRDye® 800CW	LI-COR Biosciences, Cambridge, UK.	926-32213	1:10,000	1d
Donkey anti-Goat IgG	IRDye® 800CW	LI-COR Biosciences, Cambridge, UK.	926-32214	1:10,000	1d, S4

donkey anti-rabbit IgG	Horseradish peroxidase	GE Healthcare Life Sciences, .	10794347 NA934	1:5000	6e S5c S6
sheep anti-mouse IgG	Horseradish peroxidase	GE Healthcare Life Sciences,	10094724 NXA931	1:5000	6b, 6c
Goat anti-mouse	Alexa568	Invitrogen	A-11011	1:500	1f, 1g, 4b, 5b, 7, 8b, S1g, S3b, S5e, S9a, S10b
Donkey anti-mouse	Cy5	Dianova	715-175-151	3.25µg/ml	S8b
Goat anti-mouse	Horseradish peroxidase	Advansta	R-05071-500	1:10,000	S10d
Goat anti-rabbit	Horseradish peroxidase	Advansta	R-05072-500	1:10,000	S10d

Table S9. Prokaryotic and eukaryotic expression vectors used here. Unless otherwise stated vectors allow expression of protein in mammalian cells and were generated in this study. pENTR vectors were used to generate adenoviruses ².

Vector	Expressed protein
pENTR-EGFP	EGFP alone ² .
pENTR-EGFP-C2-mm-FMN1, FH1-FH2-FSI, N-term, ΔFSI, FH2-FSI	Murine full-length FMN1 and aa849-1430, aa1-859, aa1-1394, aa985-1430 fragments as a fusion to the C-terminus of EGFP. Generated by PCR and sub-cloning from pEGFPC2-FMNiso1b (Addgene #19320) (XP_011237597) ³ .
pENTR-EGFPC1-Myc-hs-SPIRE1	Human SPIRE1 (KIAA1135) as a fusion to the C-terminus of EGFP-Myc-epitope.
pENTR-EGFPC1-Myc-hs-SPIRE2	Human SPIRE2 (AJ422077) as a fusion to the C-terminus of EGFP-Myc-epitope.

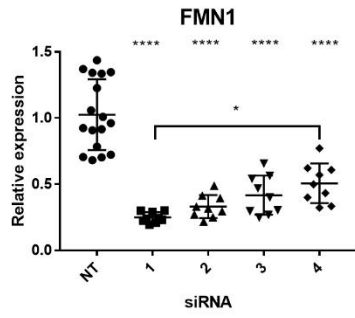
pGEX-4T1-rn-Rab27a (-WT, -Q78L, -T23N)	Wild-type, active and inactive mutant forms of rat Rab27a (P23640) in <i>E.coli</i> as fusions to the C-terminus of GST.
pcDNA3-Myc-hs-SPIRE1, KWM and MSFH	Full-length human SPIRE1 (KIAA1135), aa2-524 and aa388-742 fragments as a fusion to the C-terminus of the Myc-epitope.
pcDNA3-Myc-hs-SPIRE2 and MSFH	Full-length human SPIRE2 (AJ422077) and aa361-714 fragment as a fusion to the C-terminus of the Myc-epitope.
pAcGFP1-C1-hs-SPIRE1-MSFH, SFH, SF, FYVE and SB	Full-length human SPIRE1 (KIAA1135), aa388-742, aa525-742, aa525-697, aa573-697 and aa525-572 fragments as a fusion to the C-terminus of AcGFP1.
pCMVMYC-mCherry	Myc-mCherry fusion protein ⁴ .
pENTR-V5-vYn Myc-hs-SPIRE1 and hs-SPIRE2	Full-length human SPIRE1 and SPIRE2 as a fusion to the C-terminus of the V5 epitope tag and an N-terminus fragment (ACE74713) of Venus YFP.
pENTR-V5-vYc- rn-Rab27a, T23N, Q78L, N133I	Rat Rab27a as a fusion to the C-terminus of the V5 epitope tag and an C-terminus fragment (AM779184.1) of Venus YFP.
pAcGFP1-C1-mm-Mlph RBD	Rab27a binding domain of murine Mlph (aa 1-150; NP_443748.2) as a C-terminus fusion to GFP.
pENTR-EGFPC2-mm-MyoVa1-920aa-Syt12-a RBD	Active S1 (motor-lever) fragment of murine myosin-Va fused at the N-terminus to GFP and

	the C-terminus to the Rab27a binding domain of murine Syt12-a, described previously ⁵ .
pENTR-EGFPC2-mm-MyoVa1-920aa-SPIRE1/2	As above but with Syt12-a replaced with either murine SPIRE1 or SPIRE2. Murine SPIRE coding sequence was PCR amplified from EST clones IRAVp968A10102D (Q52KF3.1) and IRAVp968C09162D (NP_758491.1) obtained from Source Bioscience, Nottingham, UK.
pENTR-EGFPC1-hs-SPIRE2 MSFH, KW, WMSFH and KMSFH	Human SPIRE2 (AJ422077) protein fragments; aa 361-714, aa1-370, aa230-714, aa2-230 with 361-714.
pENTR-EGFPC1 hs-SPIRE2-KW-Rab27a	Human SPIRE2 (AJ422077) aa1-370 fused to the C-terminus of EGFP and the N-terminus of Rab27aSF1F4 ⁶ .
pENTR-EGFPC2-mm-FMN1-FH1-FH2-Rab27a-SF1F4	Murine FMN1 fragment aa840-1401 fused to the C-terminus of EGFP and the N-terminus of Rab27aSF1F4 ⁶ .
pENTR-EGFPN3-mm-FMN2, pENTR-EGFPC1-mm-FMN2	Murine FMN2 full length (NP_062318.2) fused to the N- and C-termini of EGFP.
pENTR-EGFPC1-mm-FMN2-FH1-FH2-FSI	Murine FMN2 aa854-1587 fused to the C-terminus of EGFP.
pEGFPC3-rn-Rab27a	Rat Rab27a as a fusion to the C-terminus of EGFP ⁷ .
pmRuby3-C1-rn-Rab27a	Rat Rab27a as a fusion to the C-terminus of mRuby3.

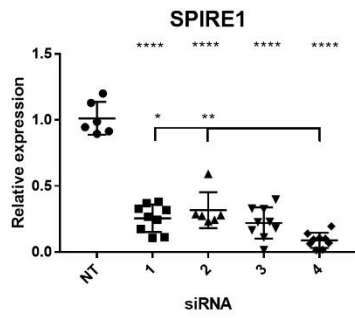
pEGFP-C2-mm-MyoVa-CC-GTD	Murine myosin Va fragment (aa 1260-1880) as a fusion to the C-terminus of EGFP ⁸ .
--------------------------	---

Supplementary Figure 1

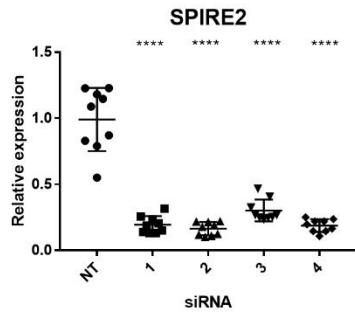
a



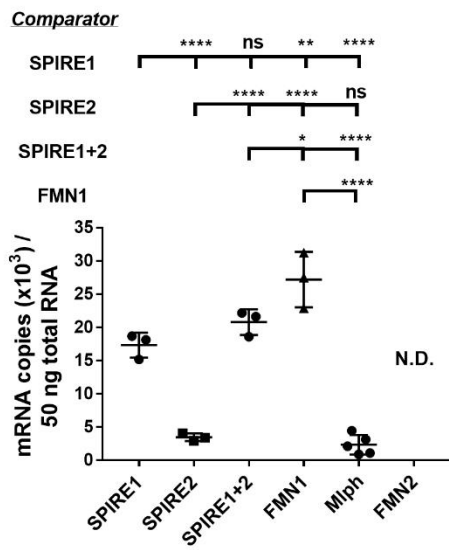
b



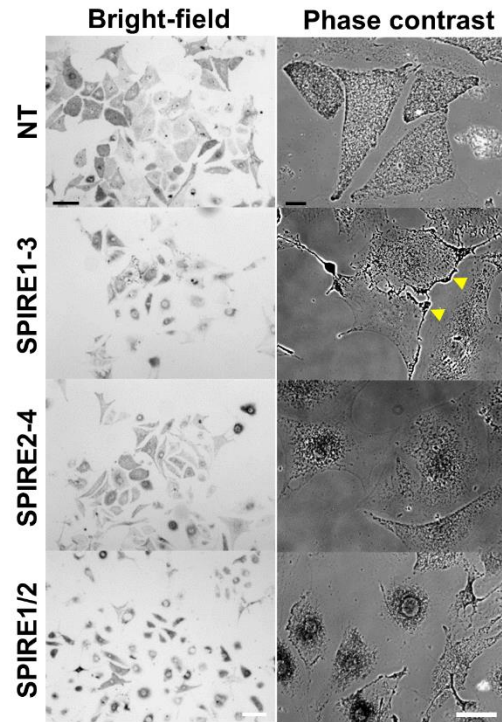
c



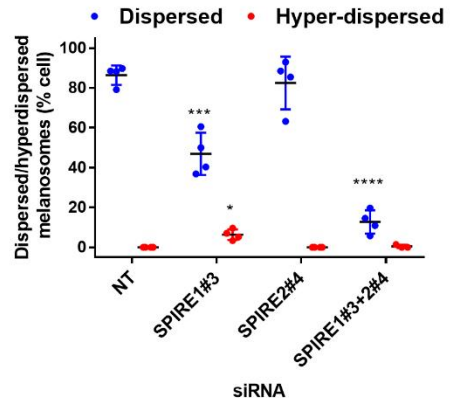
f



d



e



g

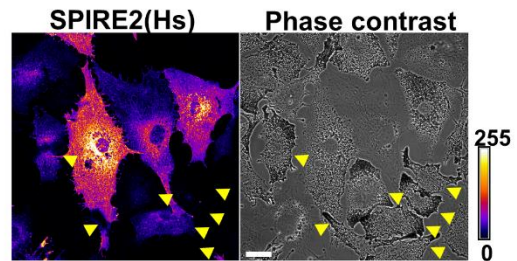


Figure S1. The effect of siRNA transfection on FMN1 and SPIRE1/2 mRNA and melanosome dispersion. **a-c)** Bee swarm plots showing the effect of transfection of melan-a cells with FMN1, SPIRE1 and SPIRE2 specific siRNA oligonucleotides on mRNA levels of the target as measured using Taqman RT-PCR (see Experimental procedures). Each point represents the Taqman assay signal normalised to the mean signal of the NT (non-targeted) control siRNA transfection. **d)** Low and high magnification images showing the distribution of melanosomes in populations of cells transfected using the indicated siRNA directed against SPIRE1 and -2 alone or in combination. Arrows in phase contrast images indicate examples of cells manifesting hyper-dispersed melanosomes. Scale bars = 100 and 20 μm for bright-field and phase contrast images. **e)** A bee swarm plot showing the percentage of siRNA transfected cells in which melanosomes are classed as dispersed or hyper-dispersed. Data are from one experiment and are representative of 3 independent experiments. **f)** A bee swarm plot showing the results of quantitative RT-PCR analysis of the expression of SPIRE1/2, FMN1/2, and MLPH genes in melan-a cells. Data are from 3 independent experiments. N.D. indicates not detected. **g)** Confocal fluorescence and phase contrast micrographs (single z-sections) show the distribution of hsSPIRE2 (displayed using 'fire' LUT to highlight cells expressing low levels of SPIRE2) and melanosomes in SPIRE1/2 depleted melan-a cells. Arrows indicate cells with hyper-dispersed melanosome distribution. Scale bar represents 20 μm . **a-c, e-f)** ****, ***, ** and * indicate significant difference $p \leq 0.0001$ and $p \leq 0.001$, $p \leq 0.01$ and $p \leq 0.05$ as determined by one-way ANOVA. No other significant differences were seen. Significance indicators at the top of each plot show significance of difference compared with NT control. Horizontal bars indicate the other pairs of data sets that showed significant differences. No other significant differences were observed. Bars indicate the mean and 25th and 75th percentile of data. Source data for **a-c, e** and **f** are provided in the supplementary Source Data file.

Supplementary Figure 2

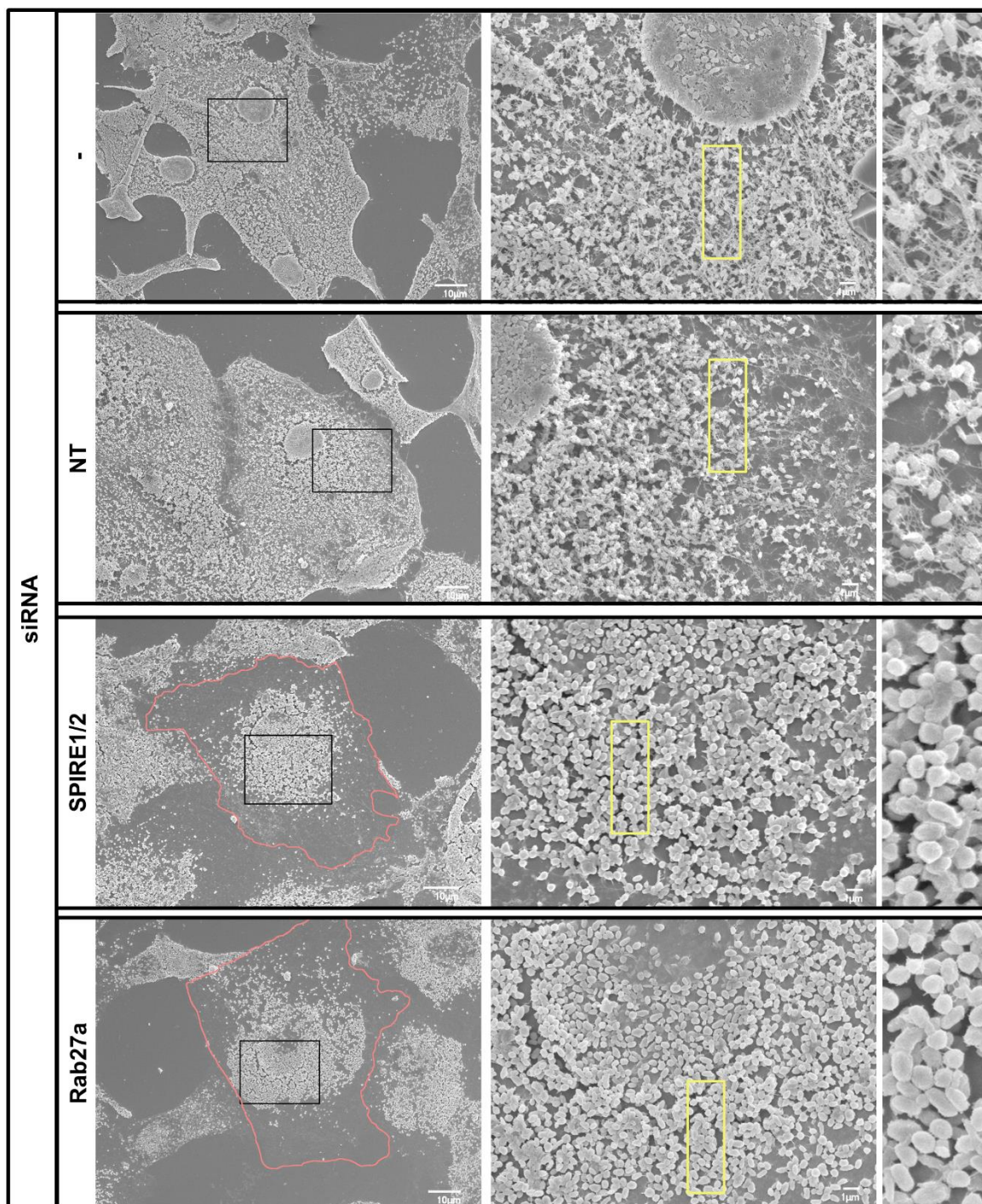


Figure S2. Scanning electron microscopy reveals a reduction in melanosome associated AFs in SPIRE1/2 and Rab27a depleted melanocytes compared with controls. Wild-type (melan-a) cells were transfected with the indicated siRNA before fixation and preparation for FESEM (see Experimental procedures). Boxes in low/medium magnification (left/central) images indicate the regions shown in high magnification images to their right. Scale bars = 10 and 1 μ m in left and central images.

Supplementary Figure 3

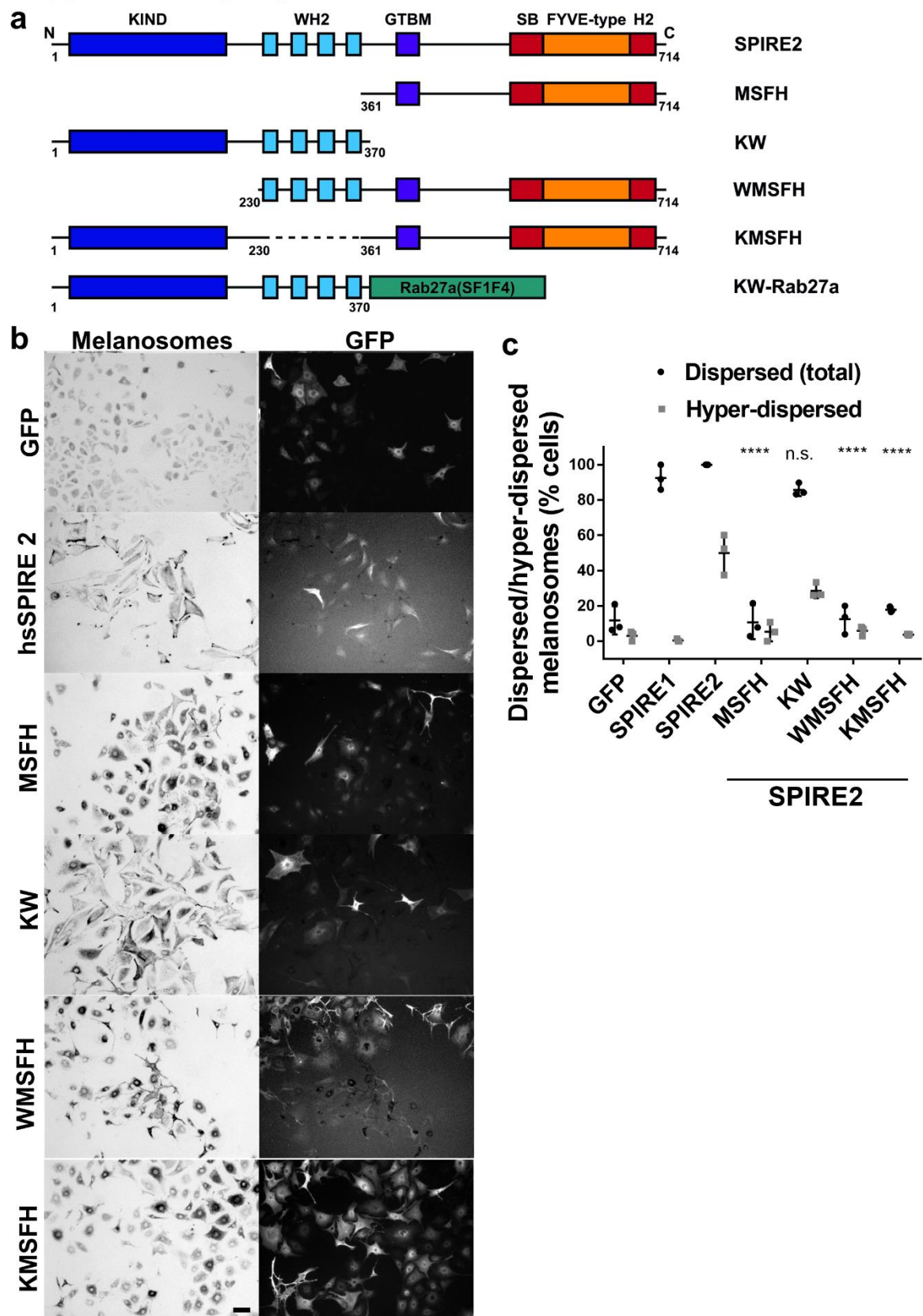
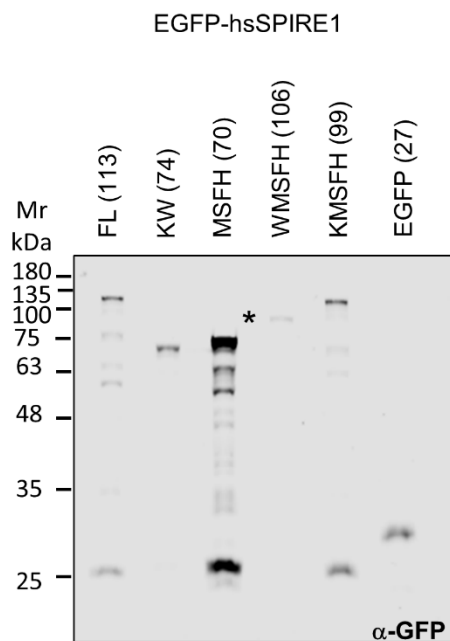


Figure S3. The FMN interaction (KIND) and AF nucleation (WH2) activities of SPIRE2 are essential for

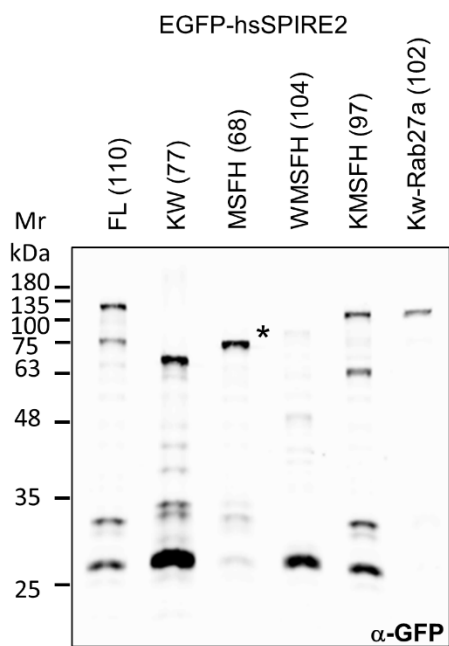
melanosomes dispersion. **a)** A schematic representation of the domain structure of human SPIRE2 and the correspondence with truncations and chimeric proteins used in functional studies (**b-c**). Numbers indicate amino acid boundaries. *K*, KIND; *W*, WH2; *M*, GTBM, globular tail domain binding motif; *S*, SB, SPIRE-box; *F*, FYVE-type zinc finger; *H*, C-terminal flanking sequences similar to H2 of Mlph-type Rab27 effectors. **b)** melan-a cells were depleted of SPIRE1/2 by siRNA transfection and 72 hours later infected with adenoviruses expressing the indicated proteins. Cells were fixed 24 hours later, processed for immunofluorescence and imaged using bright-field and fluorescence optics to observe melanosome and protein distribution/expression (see Experimental procedures). Scale bars = 50 μm . **c)** Is a bee swarm plot showing the percentage of human SPIRE2 expressing SPIRE1/2 siRNA depleted melan-a cells in which melanosomes are classed as dispersed and/or hyper-dispersed. **** and n.s. indicate significant difference $p = < 0.0001$ and no significant difference as determined by one-way ANOVA in % dispersed-type cells (total) between the test population and the control population of SPIRE2 expressing cells. Results shown are from 3 independent experiments. Bars indicate the mean and 25th and 75th percentile of data. Source data for **c** are provided in the supplementary Source Data file.

Supplementary Figure 4

a



b



c

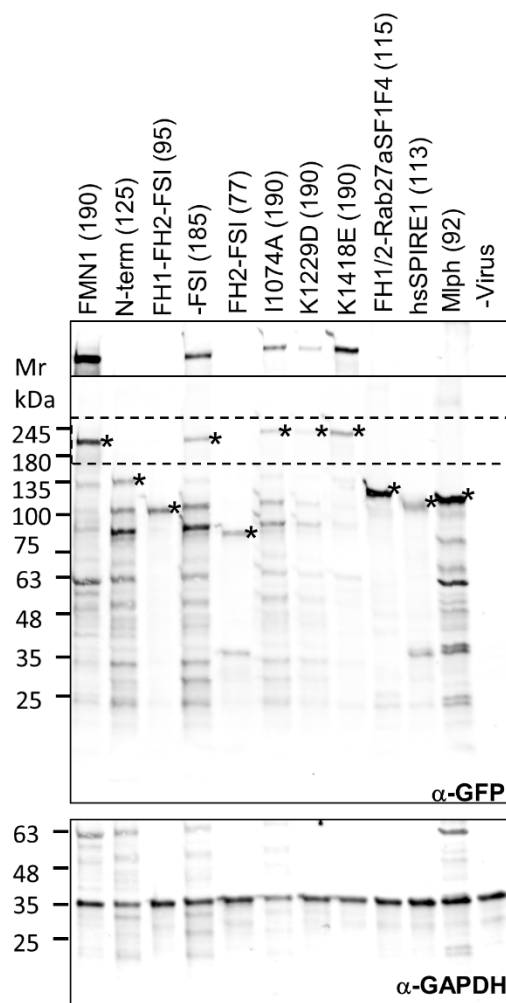
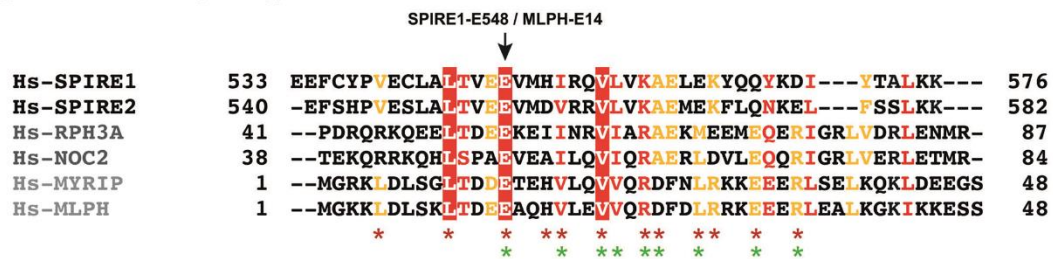


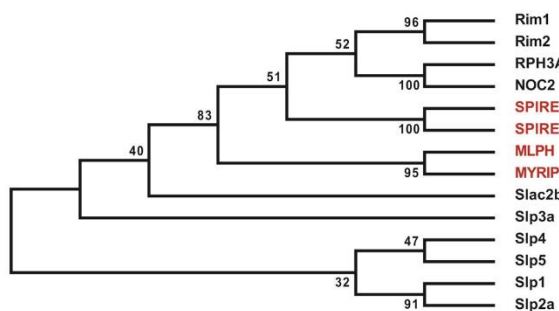
Figure S4. Confirmation of the expression of SPIRE1/2, FMN1 and mutant proteins in melanocytes. melan-a (**a-b**) and melan-f (**c**) melanocytes were infected with viruses expressing the indicated proteins as GFP fusions. Cells were harvested 48 hours later, whole cell lysates were generated and GFP fusion proteins detected by immunoblotting (see Experimental Procedures). The dotted box in **c** indicates the region shown above using a longer exposure time to improve the visibility of faint bands. Calculated molecular masses, based on amino acid sequences, are indicated in brackets adjacent to the protein name. In **c** lysates were also blotted with anti-calnexin as a loading control. Asterisks indicate the bands that are likely to correspond to each full-length GFP fusion protein based on their primary structure (**a** and **b** to the left of the band and **c** to the right on the band). Source data for **c** are provided in the supplementary Source Data file.

Supplementary Figure 5

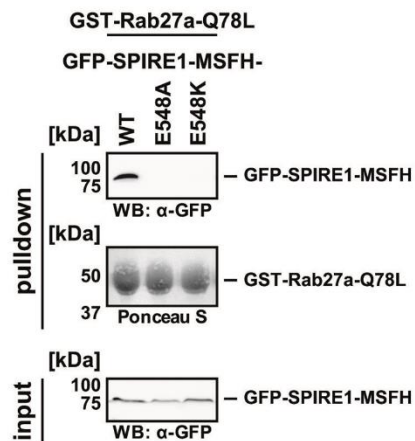
a



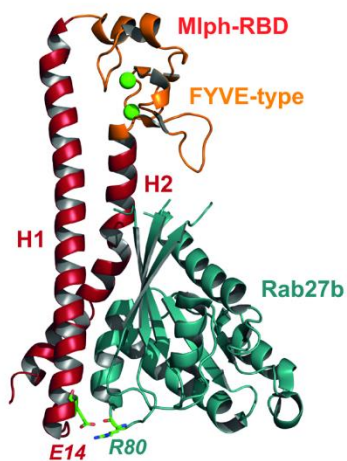
b



c



d



e

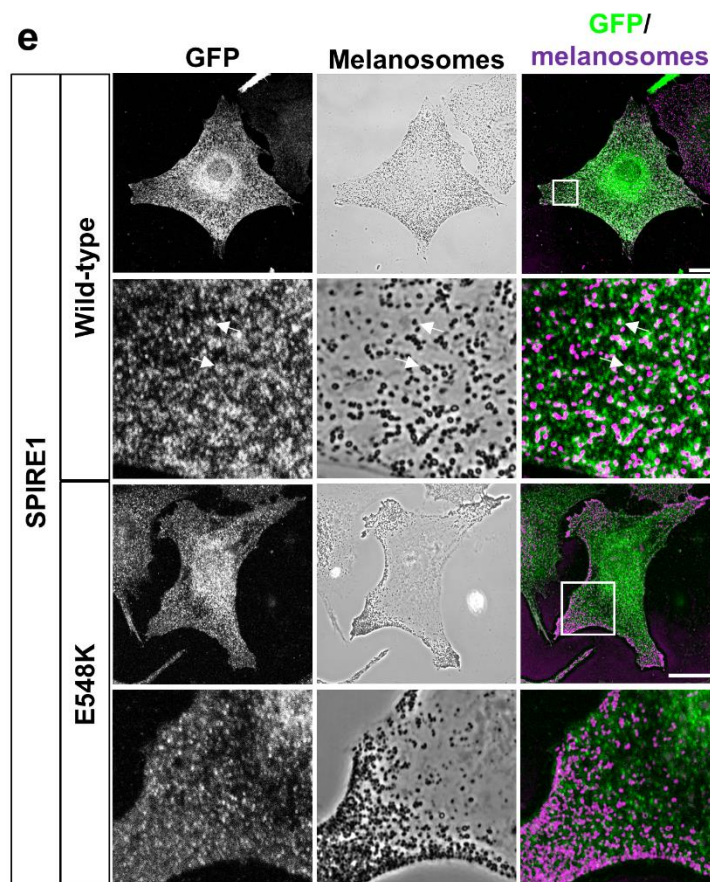


Figure S5. Comparison of the membrane binding C-terminus of SPIRE1/2 with the Rab27 binding domains of Slp/Slac effectors and generation of the Rab27 interaction deficient SPIRE1^{E548K} mutant.

a) A multiple protein sequence alignment of the H1/SB portions of human (Hs) SPIRE and the indicated Slp/Slac class Rab27/3 effectors. Asterisks below the alignment indicate contact residues of Mlph (red) and rabphilin3a (green) in complex with Rab27b and Rab3a^{9,10}. Lettering indicates residues that are highly (red) or somewhat (brown) conserved among SPIREs and other effectors. Red shaded letters are fully conserved among Rab27/3 effectors and whose replacement with alanine results in reduced SPIRE1/Rab27a interaction. Numbers on the right indicate amino acids for the respective sequence.

b) Phylogenetic tree of the Rab27 binding domains of Rab27 effectors Rim1/2, Rabphilin3A, Noc2, Mlph, Myrip, Slac2b/Exophilin, Slp1/2a/3a/4/5 and the SPIRE1 and SPIRE2 proteins (see experimental procedures for accession numbers). The evolutionary history was inferred using the *Maximum Likelihood* method based on the JTT matrix-based model. The bootstrap consensus tree inferred from 500 replicates is taken to represent the evolutionary history of the taxa analysed. Branches corresponding to partitions reproduced in less than 50% bootstrap replicates are collapsed. The percentage of replicate trees in which the associated taxa clustered together in the bootstrap test (500 replicates) are shown next to the branches.

c) A GST-pulldown assay with purified GTP-locked GST-Rab27a-Q78L and HEK293 cell lysates transiently over-expressing AcGFP1-tagged C-terminal (GFP-SPIRE1-MSFH) human SPIRE1 and mutants. Protein expression levels are shown (input) and Ponceau S staining shows equal amounts of GST-Rab27a-Q78L. N = 2-3 experimental repeats. WB = Western blotting.

d) Ribbon representation of Rab27B/Mlph-RBD complex structure (PDB ID: 2ZET) showing the position of Mlph E14 and Rab27B R80 and their possible electrostatic interaction⁹.

e) The distribution of SPIRE1 wild-type and E548K protein and melanosomes in melan-a cells. Cells expressing GFP-SPIRE1 fusion proteins were processed for confocal microscopy (see Experimental Procedures). Images are single confocal z-sections. Scale bars = 20 μm. Boxes in low magnification images (upper trio for each protein) indicate the region shown below in high magnification images.

Arrows indicate association between melanosomes and SPIRE1 protein. Source data for **c** are provided in the supplementary Source Data file.

Supplementary Figure 6

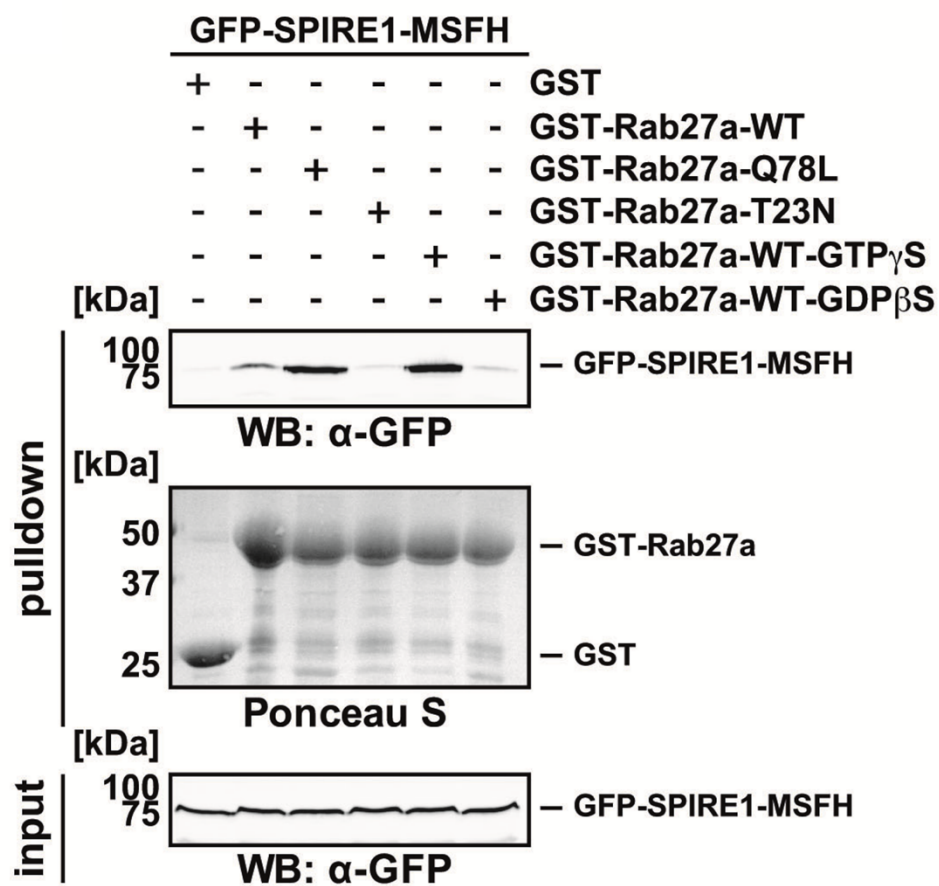


Figure S6. Nucleotide dependent interaction of Rab27a with the membrane binding C-terminus module of SPIRE1. GST-pulldown assay with purified GST-Rab27a wild-type (WT), GTP-locked (Q78L and WT-GTP γ S), GDP-locked (T23N and WT-GDP- β S), GST alone as control and HEK293 cell lysates transiently over-expressing AcGFP1-tagged C-terminal SPIRE1 (GFP-SPIRE1-MSFH). Respective protein expression levels are shown (input) and Ponceau S staining shows equal amounts of GST-Rab27a proteins. N = 2 experimental repeats. WB indicates Western blotting. Source data are provided in the supplementary Source Data file.

Supplementary Figure 7

a

MSDGDYDYLIKFLALGDSGVGKTSVLYQYTDGKFNSK**F**ITTVG
IDFREKRVVYR**ANGPDGAVGR**GQR**IHLQLWDTAGQER**FR**SLTT**
AFFRDAMGFLLLFDLTNEQSFLNVRNWISQLQMHAYCENPDIV
LCGNKSDLEDQRAVKEEEARELAEKYGIPIYFETSAANGTNISH
AIEMLLDLIMKRMERCVDK**SWIPEGVVRSNGHTSADQLSEEK**E
KGLCGC

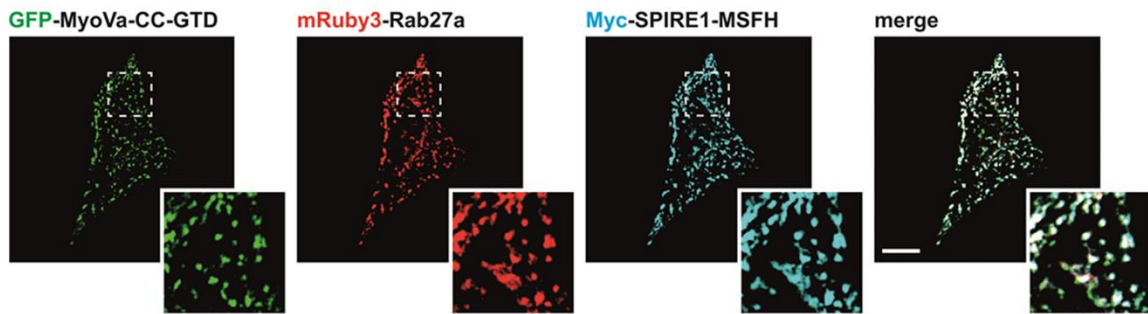
b

MAQAAGPAGGGEPR**TEAVGGEGPREPGAAGGAAGGSRDALSLE**
EILRLYNQPINEEQAWAVCYQCCGSLRAAARRRQPRHRVRSAA
QIRVWR**DGAVTLAPAADDAGEPPVAGK**LGYSQCMETEVIESL
GIIYKALDYGLKENEERELSPPLEQLIDHMANTVEADGSNDE
GYEAAEEGLGDEDEKRRKISAIRSYRDVMK**LCAAHLPTESDAPN**
HYQAVCRALFAETMELHTFLTKIKSAKENLKKIQEMEK**SDESS**
TDLEELKNADWAR**FWVQVMR**DLRNGVKLKKVQERQYNPLPIEY
QLTPYEMLMDDIRCKRYTLRKVMVNGDIPPR**LKSAHEIILDF**
IRSRPPLNPVSARKLKPTPPRPRSLHERILEEIKAEKLRPVS
PEEIRRSRLAMRPLSMSYSFDLSDVTTPESTK**NLVESSMVNGG**
LTSQTKENGLSTSQQVPAQRKKLLR**APTLAELDSSESEEETH**
KSTSSSSVSPSFPEEPVLEAVSTRKKPK**FLPISSTPQPER**RQ
PPQRRHSIEKETPTNVRQFLPPSRQSSRSLEEFYCYPVECLALT
VEEVMHIRQVLVKAELEKYQQYK**DIYTALK**KGKLCFCRTRRF
SFFTWSYTCQFCKRPVCSQCCKKMR**LPSKPYSTLP**IFSLG**PSA**
LQRGESSMRSEKPSAHHRPLRSIARFSSKSK**SMDKSDEELQF**
PKELMEDWSTMEVCVDCKKFISEIISSSRSLVLANKRARLKR
KTQSFYMSSPGPSEYCPSERTISEI

Figure S7. Sequence coverage of the unique peptides identified ($\geq 95\%$ confidence level) via mass spectrometry in Rab27a mouse (a) and SPIRE1 human (b). The peptide sequence coverage identified for each protein is high-lighted in green. Grey text is the complete protein sequence in each case.

Supplementary Figure 8

a



b

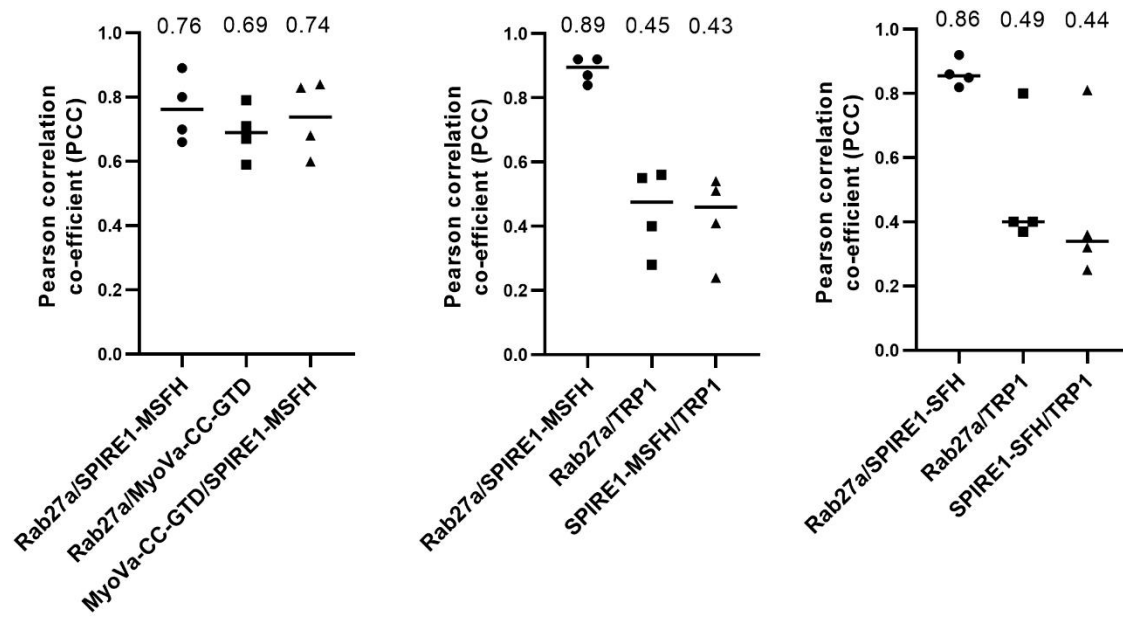


Figure S8. Colocalisation analysis of Rab27a, SPIRE1, myosin-Va and the melanosome resident

protein TRP1 in melanocytes. a) The localization of transiently co-expressed tagged MyoVa-CC-GTD (eGFP, eGFP-MyoVa-CC-GTD; green), Rab27a (mRuby3, mRuby3-Rab27a; red), and the Myc-epitope tagged (Myc, cyan) C-terminal SPIRE1 protein (SPIRE1-GTBM-SB-FYVE-H2, Myc-SPIRE1-MSFH) was analyzed by fluorescence microscopy. Deconvolved images indicate the localization of the proteins on vesicular structures. Boxes indicate regions shown in high magnification inset images. Scale bar represents 10 μm . 5 cells were recorded for each condition and one representative cell is presented here. **b)** The colocalization of tagged proteins as described in **a)** was quantified by determining the Pearson's correlation coefficient (PCC) as shown in a bar diagram (left panel). The PCC was determined for colocalization of Rab27a and C-terminal SPIRE1 proteins depending on their myosin V binding capacity (SPIRE1-MSFH, middle panel vs. SPIRE1-SFH, right panel) and the extent of localization of both, Rab27a and SPIRE1 proteins, at melanosome membranes (TRP1) was calculated. Each bar represents the mean PCC value for 4 cells analysed, mean values are indicated and error bars represent SEM. Source data for **b)** are provided in the supplementary Source Data file.

Supplementary Figure 9

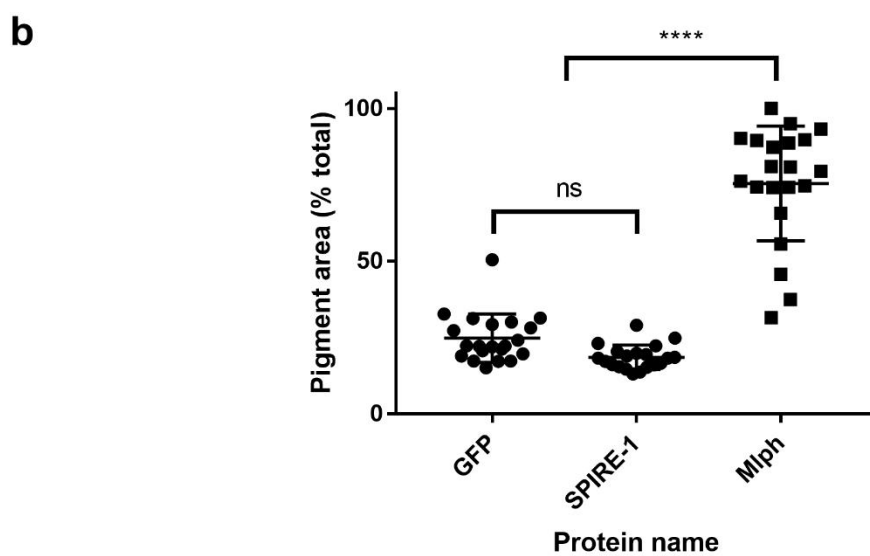
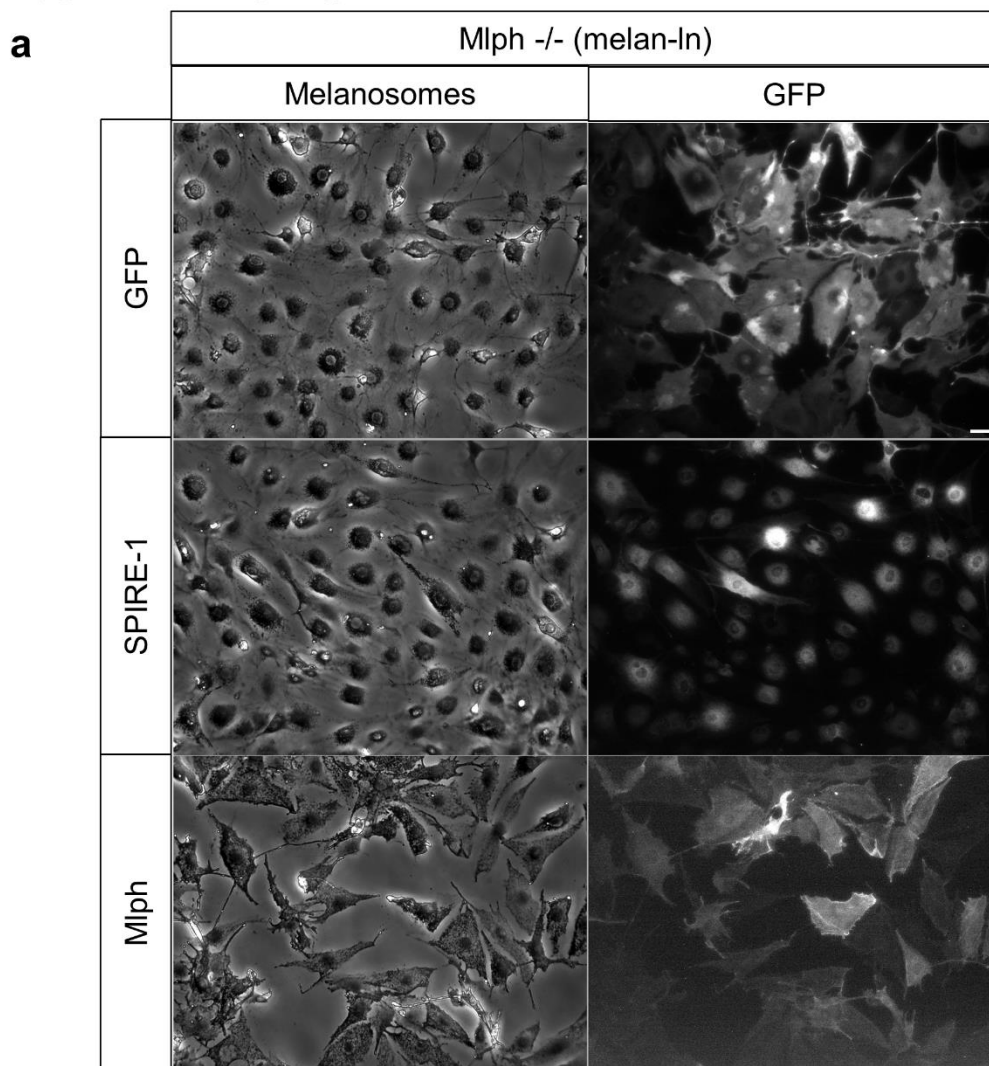


Figure S9. Expression of SPIRE1 does not restore dispersed melanosome distribution in melan-In

(Mlph -/-) melanocytes. melan-In cells were infected with adenoviruses expressing the indicated GFP fusion proteins, fixed 24 hours later, processed for immunofluorescence and imaged using phase contrast and fluorescence optics to observe melanosome and protein distribution (see Experimental Procedures). **a)** Representative images showing the distribution of melanosomes and proteins in cells. Scale bar = 20 μm . **b)** A bee swarm plot showing the extent of pigment dispersion (% total area) in cells shown in **a**. n = 20 cells for each condition. **** indicates significant difference $p < 0.0001$ as determined by one-way ANOVA. n.s. indicates no significant difference. Bars between datasets indicate the populations that are subject of statistical testing. Bars withi datasets indicate the mean and 25th and 75th percentile of data. Data shown are from one experiment and the results are representative of 3 independent experiments. Source data for **b** are provided in the supplementary Source Data file.

Supplementary Figure 10

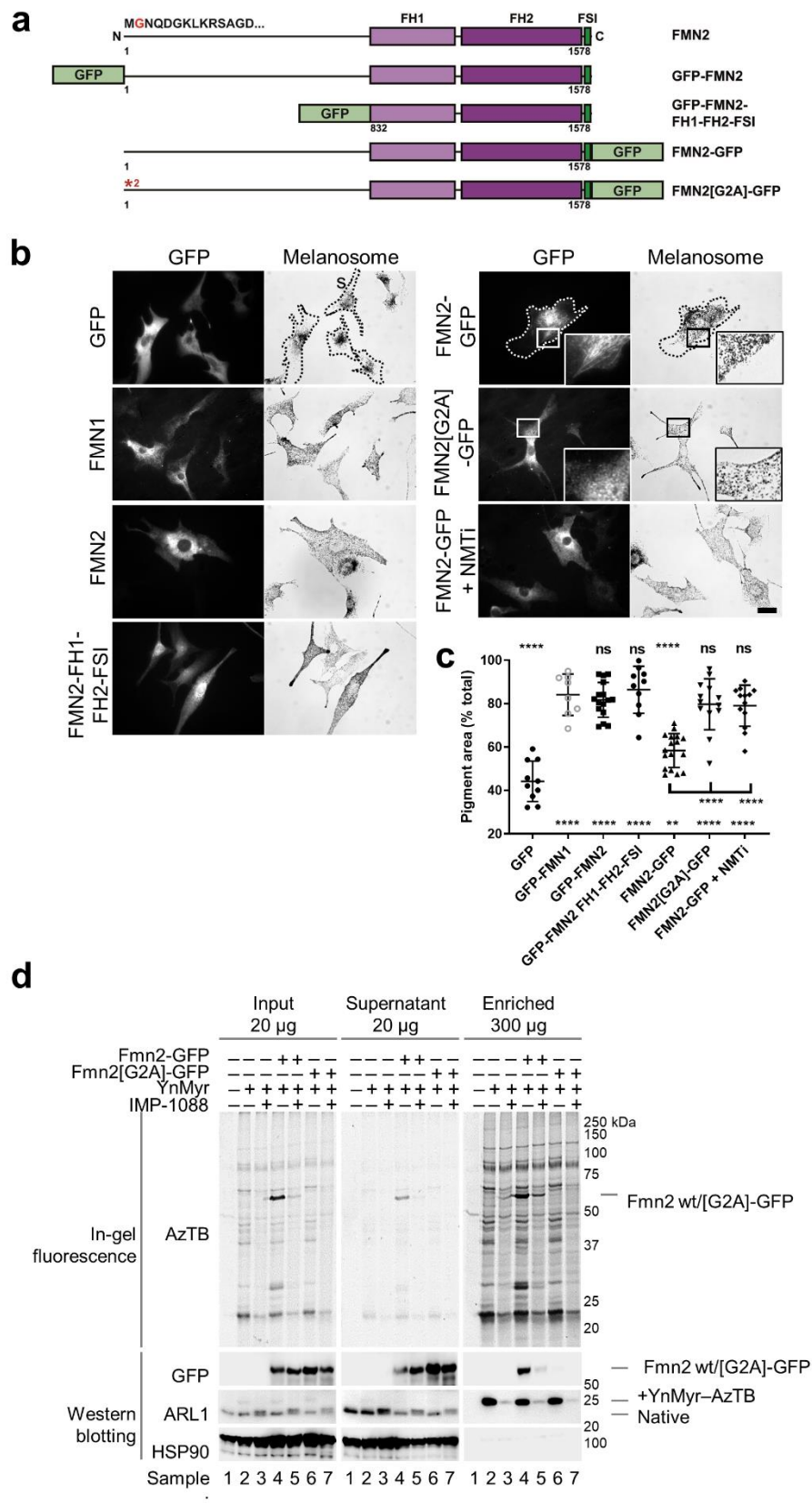


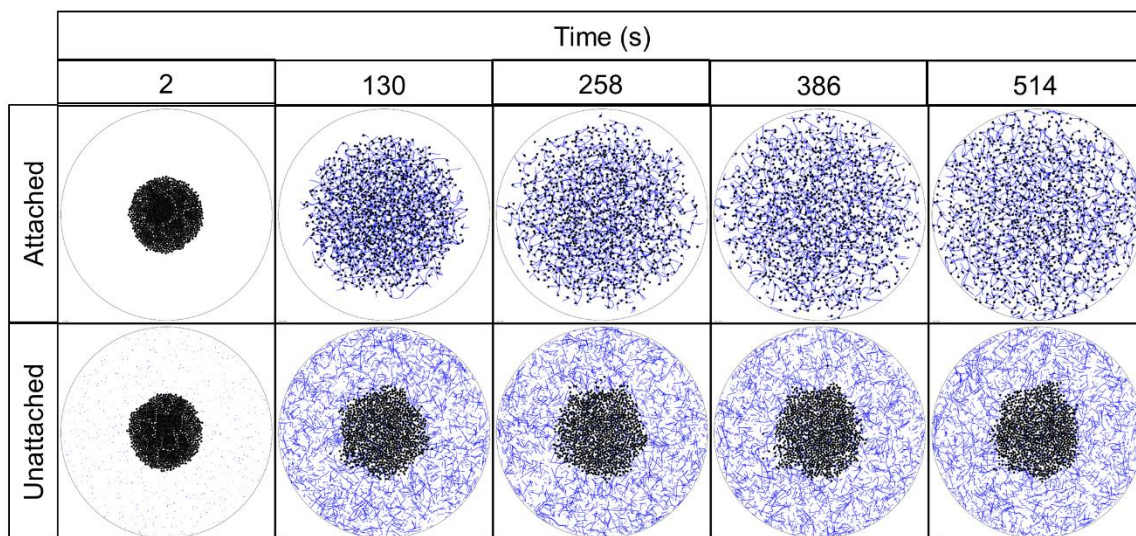
Figure S10. Perturbation of N-myristoylation of FMN2 enhances its ability to rescue melanosome

transport in FMN1 deficient melanocytes. melan-f cells were infected with adenoviruses expressing the indicated proteins in the presence/absence of NMTi IMP-1088. Cells were fixed and stained for immunofluorescence 7 hours later using anti-GFP antibodies, and the distribution of expressed protein (GFP) and melanosomes was recorded using a fluorescence microscope (see Experimental procedures). **a)** A schematic representation of the domain structure of murine FMN2 and the composition of truncations and chimeric proteins used in functional studies (**b-c**). Red text indicates the site of the glycine [2] that is predicted to undergo N-myristoylation. Numbers indicate amino acid boundaries. **b)** Representative images of cells expressing each protein. Dotted lines in FMN2-GFP images highlight the borders of cells. Scale bar represents 20 μm . **c)** A bee-swarm plot showing the extent of pigment dispersion (pigment area (% total)) in populations of cells in each condition. n (cells) = 10 (GFP), 8 (GFP-FMN1), 16 (GFP-FMN2), 10 (GFP-FMN2-FH1-FH2-FSI) 17 (FMN2-GFP), 13 (FMN2[G2A]-GFP) and 13 (FMN2-GFP + NMTi (IMP-1088 100nM)). **** and ** indicate significant difference $p = < 0.0001$ and $p = < 0.01$ as determined by one-way ANOVA. n.s. indicates no significant difference. Significance indicators above and below the dataset indicate differences between each condition and the positive (GFP-FMN1) and negative (GFP alone) controls. Horizontal bars linking dataset indicate other pairs of populations that show statistically significant differences. Results shown are representative of 3 independent experiments. Bars within datasets indicate the mean and 25th and 75th percentile of data. *FH*, formin homology; *FSI*, Formin-SPIRE interaction sequence. **d)** Purification of myristic acid analogue (YnMyr) labelled FMN2 proteins confirms N-myristoylation and the efficacy of inhibition strategies. HEK293a cells were transfected with plasmid vectors allowing expression of Fmn2-GFP and Fmn2[G2A]-GFP in the presence and absence of myristate analogue (YnMyr) and NMTi (IMP-1088). Cells were harvested 24 hours later and the myristoylated proteins purified (see Experimental procedures). Lysates (input), purified (enriched) and non-purified (supernatant) fractions were resolved by SDS-PAGE and YnMyr incorporation detected by in-gel fluorescence. Western blotting using antibodies specific for GFP shows expression of

Fmn2/Fmn2[G2A] and ARL1 and HSP90 antibodies confirm the efficacy and specificity of the labelling strategy. Source data for **c** and **d** are provided in the supplementary Source Data file.

Supplementary Figure 11

a



b

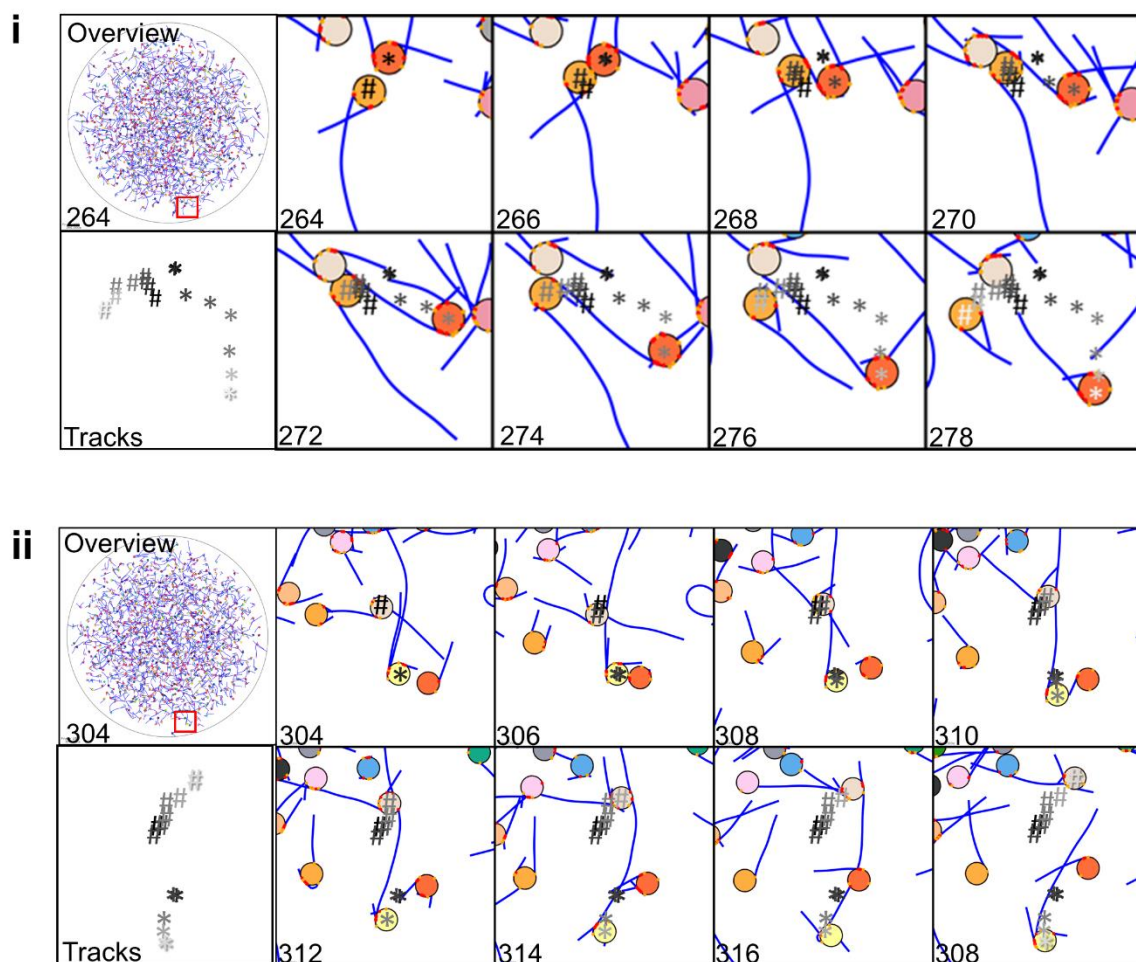


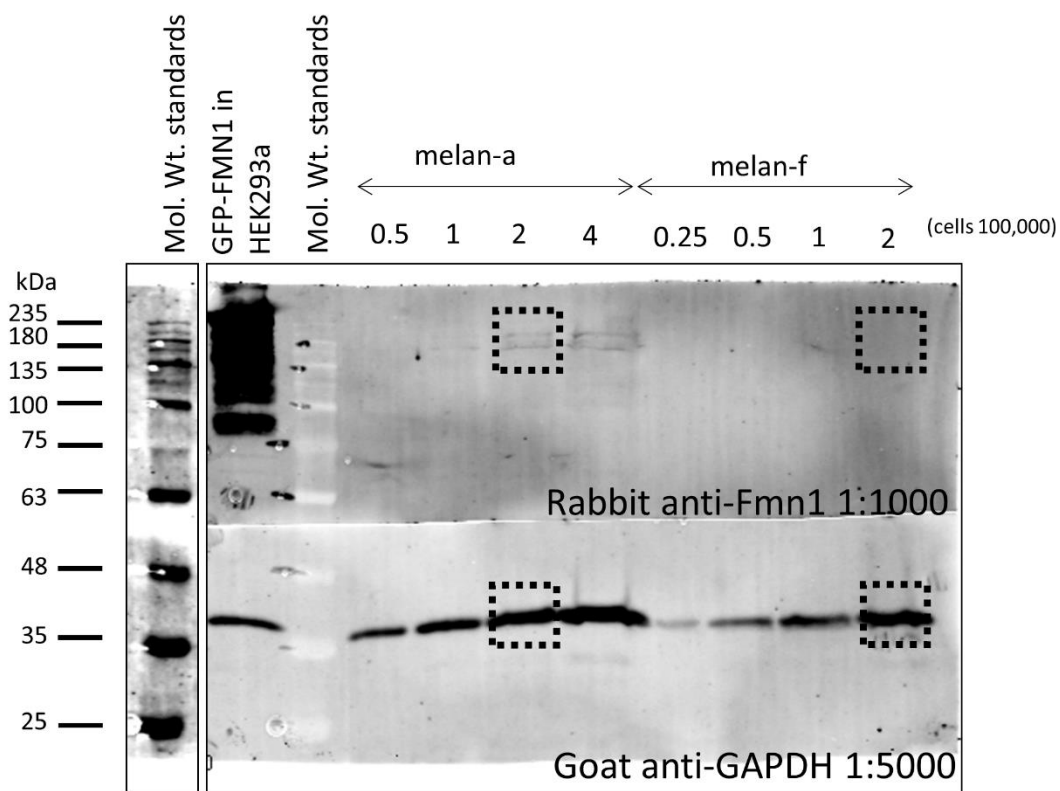
Figure S11. Simulation showing the effect of AF polarity and anchoring on melanosome transport.

Images collected from Cytosim simulations of melanosomes transport in model cells in with differing AF organisation (time from initiation of simulation is shown). Large black circles (diameter $46\mu\text{m}$), small solid black circles (diameter $0.5\mu\text{m}$) and blue lines, respectively represent the cell membrane, melanosomes and actin filaments. **a)** Attached and unattached image series show the results of transport simulations in which AF organisation is a) as described in Figure 9, i.e. with melanosomes attached via their -/pointed end to melanosomes with +/barbed ends grow outwards into the cytoplasm or b) with AFs unattached from melanosomes and free to diffuse throughout the cytoplasm. **b)** i and ii are enlarged areas ($5 \times 5\mu\text{m}$) of cytoplasm (see red box in overview image for an indication of the position of the enlarged area within the cell area) from the 'attached' simulation showing examples of local dispersal of melanosomes at different time-points. In these images each melanosome has a different colour to aid tracking of individuals over time. Myosins, attached to melanosomes, are displayed as either red or orange depending on whether they are bound or unbound from actin filaments. Hash and asterisks indicate the centre of each melanosome over time with a gradient of colour from black to light grey indicating the changing position from early to late time-points. The complete tracks for each tracked melanosome are displayed in the tracks panel. Numbers in each panel indicate the elapsed time in seconds from the start point.

References.

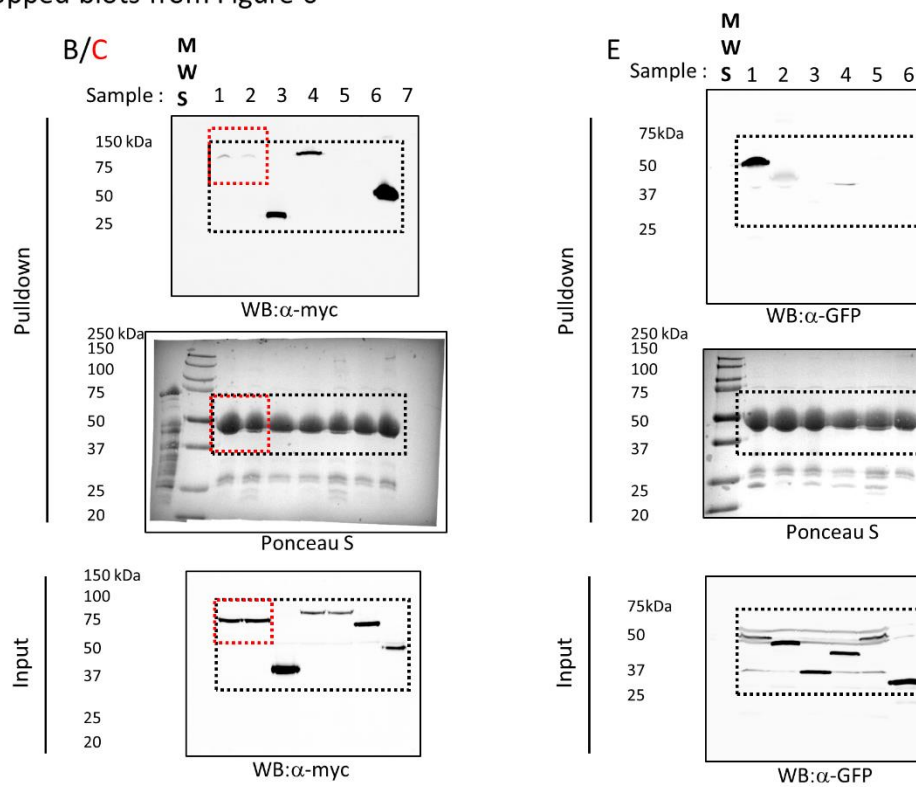
- 1 Dettenhofer, M., Zhou, F. & Leder, P. Formin 1-isoform IV deficient cells exhibit defects in cell spreading and focal adhesion formation. *PLoS One* **3**, e2497, doi:10.1371/journal.pone.0002497 (2008).
- 2 Hume, A. N., Tarafder, A. K., Ramalho, J. S., Sviderskaya, E. V. & Seabra, M. C. A coiled-coil domain of melanophilin is essential for Myosin Va recruitment and melanosome transport in melanocytes. *Mol Biol Cell* **17**, 4720-4735, doi:10.1091/mbc.E06-05-0457 (2006).
- 3 Zhou, F., Leder, P. & Martin, S. S. Formin-1 protein associates with microtubules through a peptide domain encoded by exon-2. *Exp Cell Res* **312**, 1119-1126, doi:10.1016/j.yexcr.2005.12.035 (2006).
- 4 Nightingale, T. D., Pattni, K., Hume, A. N., Seabra, M. C. & Cutler, D. F. Rab27a and MyRIP regulate the amount and multimeric state of VWF released from endothelial cells. *Blood* **113**, 5010-5018, doi:blood-2008-09-181206 [pii]10.1182/blood-2008-09-181206 (2009).
- 5 Evans, R. D. *et al.* Myosin-Va and dynamic actin oppose microtubules to drive long-range organelle transport. *Curr Biol* **24**, 1743-1750, doi:10.1016/j.cub.2014.06.019 (2014).
- 6 Tarafder, A. K. *et al.* Rab27a targeting to melanosomes requires nucleotide exchange but not effector binding. *Traffic* **12**, 1056-1066, doi:10.1111/j.1600-0854.2011.01216.x (2011).
- 7 Hume, A. N. *et al.* Rab27a regulates the peripheral distribution of melanosomes in melanocytes. *J Cell Biol* **152**, 795-808 (2001).
- 8 Strom, M., Hume, A. N., Tarafder, A. K., Barkagianni, E. & Seabra, M. C. A family of Rab27-binding proteins. Melanophilin links Rab27a and myosin Va function in melanosome transport. *J Biol Chem* **277**, 25423-25430, doi:10.1074/jbc.M202574200 (2002).
- 9 Kukimoto-Niino, M. *et al.* Structural basis for the exclusive specificity of Slac2-a/melanophilin for the Rab27 GTPases. *Structure* **16**, 1478-1490, doi:10.1016/j.str.2008.07.014 (2008).
- 10 Ostermeier, C. & Brunger, A. T. Structural basis of Rab effector specificity: crystal structure of the small G protein Rab3A complexed with the effector domain of rabphilin-3A. *Cell* **96**, 363-374 (1999).

Uncropped blot from Figure 1d



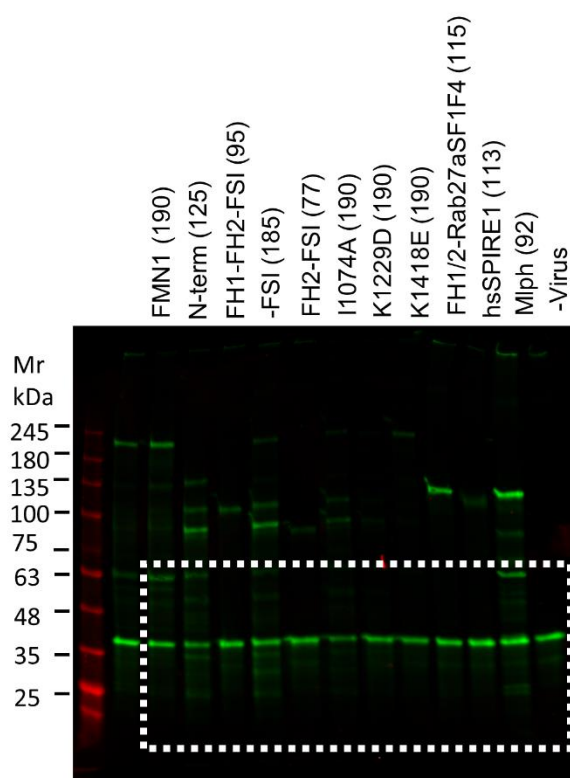
Boxes indicate the regions of the image that are included in Figure 1d

Uncropped blots from Figure 6



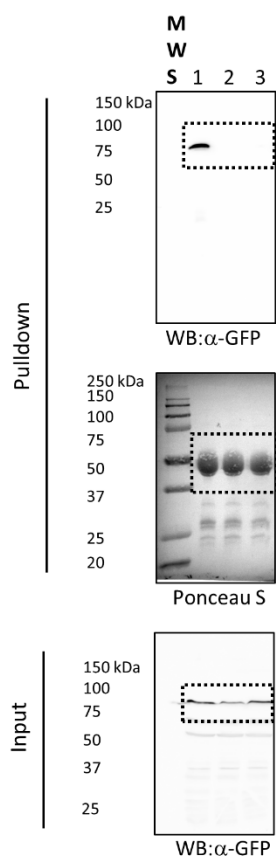
Full scans of blots and filters shown in Figure 6b, c and e. Black and red boxes indicate the areas shown in the final figure.

Uncropped blot from Supplementary Figure 4c (GAPDH)



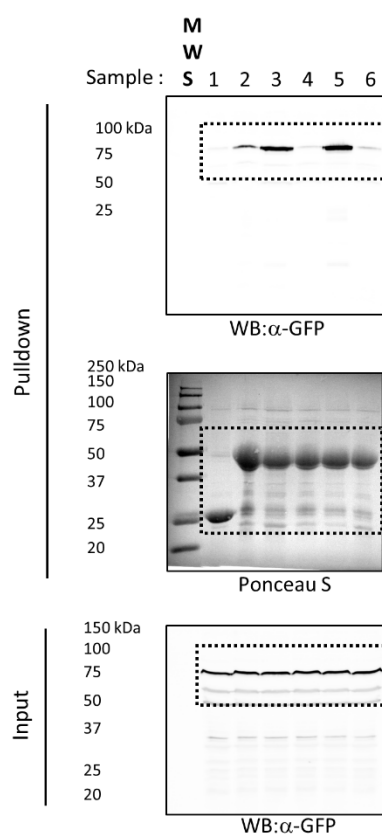
A composite image of the whole membrane showing the distribution of expressed GFP fusion proteins (bands of Mol. Wt. > 63kDa) and endogenous GAPDH (Mol. Wt. ~ 35kDa) in cell lysates (green signal) and the coomassie stained markers (red signal). The blot was probed sequentially with anti-GFP and then anti-GAPDH. The boxed area indicates the region of the image that is included as an inverted, contrast enhanced, grayscale image) in portion of Supplementary Figure 4c (GAPDH).

Uncropped blots from Supplementary Figure 5c



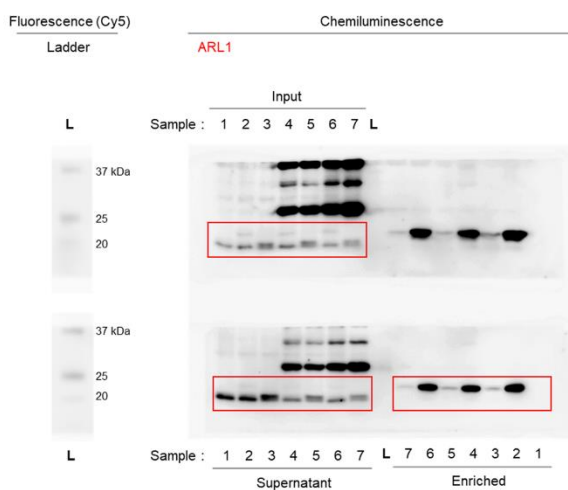
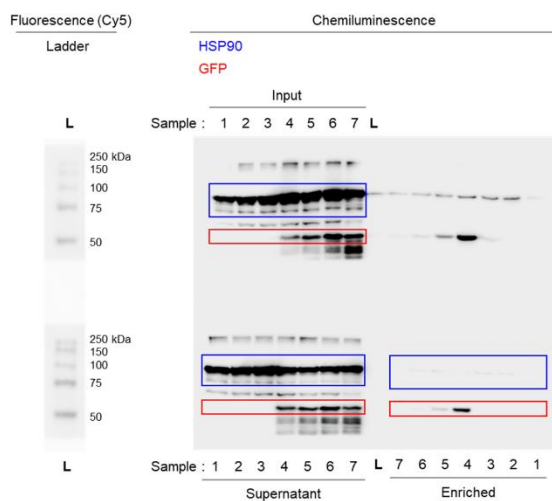
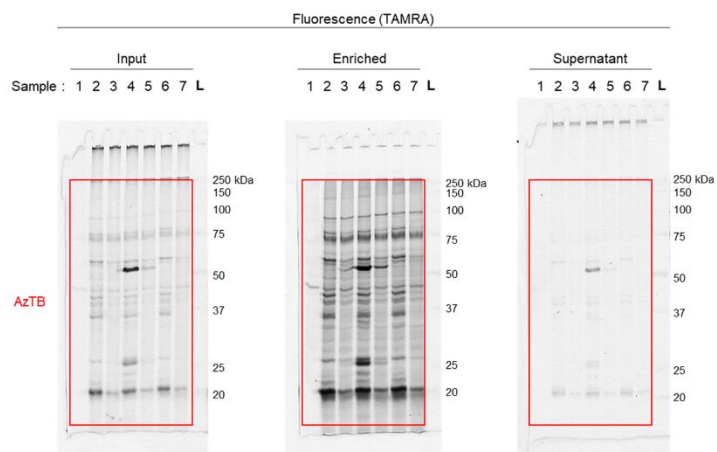
Full scans of blots and filters shown in Supplementary Figure 5c. Boxes indicate the areas shown in the final figure.

Uncropped blots from Supplementary Figure 6



Full scans of blots and filters shown in Supplementary Figure 6. Boxes indicate the areas shown in the final figure.

Uncropped blot from Supplementary Figure 10d.



Red and blue boxes indicate the areas shown in final figures.